Indian Journal of Pure & Applied Physics
Vol. 64, February 2026, pp. 181-196
DOI: 10.56042/ijpap.v64i2.25886

A Bio-Inspired Gazelle Optimization Algorithm for Parameter Tuning of Coordinated PSS-SSSC to Damp Low-Frequency Oscillation in Power Systems

Sritosh Kumar Sahoo[a], Manoj Kumar Kar[b*], Sanjay Kumar[a] & Rabindra Nath Mahanty[a]

[a]Department of Electrical Engineering, National Institute of Technology, Jamshedpur 831 014, India

[b]Department of Electrical & Electronics Engineering, Tolani Maritime Institute Pune, Maharashtra 410 507, India

Received: 24th November 2025; accepted: 31st December 2025

This study presents a novel Gazelle optimization algorithm that improves power system stability by damping low-frequency oscillations. The Gazelle optimization algorithm (GOA) optimizes the controller parameters of coordinated PSS and SSSC controllers, with the main objective of reducing rotor speed deviation. The GOA effectiveness was validated with its benchmark functions and demonstrated in a multi-machine power system as a test system. A statistical analysis has been carried out with different benchmark functions to demonstrate the superiority of the suggested algorithm along with three other optimization techniques, which are the sinecosine algorithm, moth-flame algorithm and ant lion optimization algorithm. A nemenyi hypothesis test was implemented to determine the lowest mean rank, along with the Wilcoxon signed-rank test, which shows the effecacy of the proposed algorithm. The results, which are backed by statistical analysis, demonstrate that the suggested GOA approach performs better than three alternative heuristic algorithms. The GOA-tuned parameters are finally implemented with a multimachine power system network as a test system. Different parameters, such as speed deviation between different machines, voltage injected by SSSC, and tie-line power, are compared with three other optimization techniques in the results section. From the result analysis, it has been concluded that the proposed Gazelle optimization algorithm gives superior performance than others, which proves its real-time applicability in the modern power system world.

Keywords: PSS, SSSC, MMPS, GOA-ITAE

1 Introduction

A power system is a complex interconnected system in which the stability of voltage and power flow are crucial parameters. When a generator trips or switches to a large industrial load, it can cause a significant disruption. It may cause severe disturbance, such as congestion of power flow in transmission lines, an increase in voltage, or the development of electromechanical oscillations between various system components. Modern Flexible AC Transmission Systems (FACTS) provide a solution to such problems, using power electronics. These devices are high-speed controllers that can dynamically control key electrical parameters of the grid, including transmission line impedance, voltage magnitude, and phase angle. By the use of the FACTS controllers, the flow of active and reactive power can be controlled, which in turn allows the damping of oscillations in the power system and the elimination of voltage collapse and, consequently, of the stability of the power system after a disturbance which creating greater security and reliability to the grid. These intelligent electronic gadgets, rather than slow, mechanical past switches, can react in milliseconds to instantly divert power, even out hazardous oscillations and deal with jams. With the recent improvements in power electronics, we are now in a position to add smart devices to our power grids, and they are called FACTS. This innovation is a game-changer in modern power systems, as it improves the overall stability of the power system. The stability of a multi-machine power system is essential in ensuring a stable delivery of electricity, particularly when the system is experiencing disturbances. Multi-layered networks have a tendency to oscillate at low frequency, with the generators moving in opposite directions, and this can cause outages across large-scale networks. To overcome this, PSS are conventionally installed on generators to damp these swings by varying the excitation in the generator. But as the grid becomes more complex, the usefulness of PSS alone may not be sufficient. This has seen the addition of state-of-the-art FACTS equipment, e.g. the SSSC. The SSSC can change power flow quickly and improve system

*Corresponding author: E-mail: manojkumark@tmi.tolani.edu

stability by injecting a controllable voltage in series with the transmission line. Hence, the combined use of the PSS and SSSC controllers is a strong and resilient approach. The localized damping action of the PSS is complemented by the rapid, network-wide control of the SSSC to enhance the dynamic stability and the overall security of multi-machine systems.

1.1 Literature Review

The capacity of an electric power system to maintain an operating state of equilibrium under typical operating conditions and to return to a satisfactory state of equilibrium following a disturbance is known as power system stability. Rotor angle stability refers to the ability of interconnected synchronous generators to remain in synchronism with one another after a disturbance. This study is separated into two sections: transient stability, which deals with the system's ability to tolerate big, unexpected events like transmission line faults, and small-signal stability, which deals with oscillations from small, daily fluctuations[1]. An important component of the FACTS family, the SSSC, which increases power system stability by changing the effective impedance of the line and allows dynamic power flow regulation by injecting a regulated series voltage with the line current[2]. This study presents a technique for scheduling an SSSC damping controller to minimize low-frequency oscillations in a power system. This research work demonstrates that a modified Zebra Optimization Algorithm (mZOA) is superior to the conventional ZOA and PSO algorithms in terms of controller parameter to enhance power system stability[3]. This research work represents the Gazelle Optimization Algorithm (GOA), a novel approach to difficult problem solving that draws inspiration from gazelles' grazing (exploitation) and predator-evasion (exploration). The efficacy of the GOA was confirmed through testing against engineering difficulties and benchmark functions, where it outperformed or was competitive with nine other algorithms that were already in use[4]. This study compares the tuning methods of Phase Compensation and Integral of Squared Error (ISE) to examine PSS performance. It examines the effects of series compensation, AVR transient gain reduction, and excitation systems on PSS tuning and system robustness across a range of operational loads and significant disturbances[5]. This study compares converter-based SSSC with impedance-based CSC and finds that SSSC provides better power flow regulation, particularly in lines with low loads. Furthermore, simulations show that, in some situations, SSSC is more successful than CSC at damping power oscillations[6]. This paper suggests optimizing the settings of coordinated (PSS) and SSSC damping controllers in multimachine power systems using the Salp Swarm Algorithm (SSA). With a mean value of 0.000601 pu, the goal of limiting rotor speed variation was accomplished. The SSA-tuned controllers performed better than other optimization techniques in improving system stability, especially in speed deviation, injected voltage, and tie-line power, according to MATLAB simulations[7]. In order to improve power system stability, this work optimizes PSS and SSSC controller tuning using an Improved Sine Cosine Algorithm (ISCA). Reducing rotor speed variations in a single machine infinite bus (SMIB) system is the main objective. Compared to the conventional SCA, the suggested ISCA performs better and is more resilient to a range of loads and defects[8]. In order to reduce power system oscillations in multi-machine systems under fault situations, this study compares SSSC and TCSC controllers when utilized in conjunction with Power System Stabilizers (PSS). The findings demonstrate that the PSS-assisted SSSC controller improves overall system stability by damping these oscillations faster and more efficiently than the PSS-assisted TCSC[9]. The purpose of this study is to increase the damping of particular electromechanical modes in multimachine systems by proposing a BAT search technique for the optimum design of Power System Stabilizers (PSSs). across comparison to Genetic Algorithms (GA) and Conventional PSSs, the suggested BAT-based PSS showed better performance and resilience across a range of operational scenarios and disruptions[10]. In this work, a linearized model and nonlinear optimization are used to simultaneously tune FACTS and PSS damping controllers in multi-machine power systems. The strategy works well for coordinating several controllers in big power systems, according to simulation data[11]. This study tunes SSSC and PSS damping controllers by analyzing faults (LLLG, LG, etc.) on a SMIB system using an improved sine–cosine algorithm (ISCA). By successfully lowering rotor speed deviation and suppressing oscillations under a range of fault and loading circumstances, the results demonstrate that this ISCA-tuned technique offers greater stability[12]. This work suggests a hybrid PSO–GSA algorithm-optimized coordinated PSS and SSSC damping controller that greatly enhances power

system stability by offering improved oscillation damping, even while taking system delays into account. Under a variety of circumstances, the design is reliable and efficient in systems with one or more machines[13]. To optimize PSS and SSSC controller tuning for improved power system stability, a Modified Sine Cosine Algorithm (MSCA) that combines exploration (SCA/rand-target) and exploitation (SCA/best-target) is suggested. When tested on SMIB and MMPS systems, MSCA dramatically lowers rotor speed deviation and system oscillations, outperforming other heuristic algorithms in terms of performance and resilience[14]. In order to improve power system stability and lessen fluctuations under disturbances including three-phase faults and uneven loads, this research offers an optimized Static Synchronous Series Compensator (SSSC) system employing a Fuzzy Controlled Differential Evolution (FCDE) method. When compared to other optimization methods (PSO, Genetics, DE, GSA) in simulation, the FCDE-integrated SSSC model significantly increased performance and stability[15]. Using SMIB models, this work suggests constructing PSS for a N-machine system based on the discovery that the least-damped mode in analogous constructed identical-machine systems is less damped than the modes of the N-machine system. It is demonstrated that this SMIB-based design enhances the electromechanical oscillation damping of the entire N-machine system[16]. In order to improve power system stability, this study suggests using the Modified Grey-Wolf Optimization Algorithm (MGWOA) to adjust Fractional-Order PID (FOPID) damping controllers (Power System Stabilizer/Static Synchronous Series Compensator). The MGWOA approach, which was tested on SMIB and MMPS systems, reduces rotor speed deviation and outperforms existing heuristic methods in attenuating low-frequency oscillations[17]. In order to adjust the Power System Stabilizer (PSS) parameters in a multi-machine system, this study suggests and assesses four variations of a population-based Grey Wolf Optimization (GWO) algorithm: MGWO, MGWOPSO, MGWOSCA, and MGWOCSA. By optimizing an objective function that increases damping ratios and moves system eigenvalues to the left on the s-plane, the purpose is to dampen low-frequency oscillations. The enhanced performance is confirmed by statistical tests and comparative analysis[18]. This study describes an MGWOA-tuned Fractional-Order PID controller for a SMIB system integrating with SSSC. The proposed controller suppresses the oscillations and gives superior performance compared to other algorithms[19]. Using the PSO metaheuristic technique, this paper suggests a PSS tuning methodology for large electric power systems (ten or more machines). The method was successfully applied in DigSilent PowerFactory and proved to be successful on a number of test systems[20]. In order to solve the low convergence accuracy and instability of the Gazelle Optimization Algorithm (GOA), this study presents the MPSOGOA algorithm, which combines Particle Swarm Optimization (PSO) with GOA and employs chaos mapping for improved population initialization. MPSOGOA outperforms other metaheuristic algorithms in terms of convergence accuracy and stability when tested on 35 engineering and benchmark tasks[21]. This study introduces MGWPSO, a novel optimization technique to enhance power system stability. The technique efficiently reduces rotor speed changes and dampens oscillations by fine-tuning control parameters for devices such as PSS and SSSC. Statistical testing and real-time simulations verify that this hybrid strategy improves power system control more effectively than other cutting-edge methods[22]. In order to address problems with the original Gazelle Optimization Algorithm, such as an inadequate balance between exploration and exploitation, this study presents the Multi-Strategy Improved Gazelle Optimization Algorithm (MSIGOA). On benchmark tests, MSIGOA outperforms the basic GOA and other sophisticated algorithms in terms of performance, convergence, and efficiency by employing an iteration-based updating framework and other novel techniques[23].

1.2 Novelty and the Structure of the Paper

i A new metaheuristic optimization, i.e. the Gazelle Optimization Algorithm (GOA), is introduced first time in this field of research for fine-tuning the parameters of the controller to achieve optimum results.

ii A statistical analysis was performed to verify the reliability of the proposed GOA. The efficacy of the proposed algorithm was tested on both unimodal and multimodal functions, and its results were benchmarked against three other recent effective optimizers: SCA, MFO, and ALO.

iii For a comparative statistical analysis, the Friedman and Nemenyi hypothesis tests were

used along with the Wilcoxon signed-rank test, which established a mean performance rank and paired t-test for each of the algorithms, respectively.

iv The GOA optimized controller parameters were applied to MMPS power systems across various load scenarios to improve the performance. The different findings, including the mean, standard deviation, and optimal parameters of the suggested GOA, are thoroughly analyzed and compared with three other optimization methods.

2 System Description

2.1 Multimachine Power System (MMPS)

The System shown in Fig. 1 is a Multi-Machine Power System (MMPS) which contains three generators, six buses and four energy loads. The total system forms two subsystems, which are connected by a tie-line. A three-phase fault between buses 2 and 6 causes system instability with power oscillations. To maintain stability, two control mechanisms are used; SSSC is connected between buses 5 and 6, and each generator is equipped with a PSS. The coordinated way of the SSSC and the PSS working is to dampen the local and inter-area power swings effectively, thus increasing the overall stability of the system.

2.2 Power System Stabilizer

The Fig. 2 shows the block diagram of a conventional Power System Stabilizer (PSS). The main purpose of PSS is to maximise the damping of electromechanical oscillations of low frequency in a power system. The speed deviation, Δw, of the generator is taken as input, and the corresponding supplementary stabilizing voltage signal, Vs, is produced as the output of the system. This output signal is then fed into the generator's excitation system for the purpose of damping any oscillations. It consists of three main blocks, i.e. a gain block, a washout block and a two-stage lead-lag block.

2.2.1 Gain Block

The function of the gain block is to set the overall strength of the stabilizer's response by scaling the magnitude of the incoming speed deviation signal.

2.2.2 Washout Block

This block acts as a high-pass filter, which allows the system to respond to rapid oscillations while disregarding slow, steady operational changes in speed.

2.2.3 Two-stage lead-lag Block

This circuit compensates the signal timing aspect to offset the delays that are inherent to the generator system so that the corrective act can be applied at the most opportune time to tame the power swings.

2.3 Static Synchronous Series Compensator

To enhance the stability of the power system, a special damping controller is used, which injects the voltage (Vq) by SSSC into the grid. This controller is constructed out of three core components: a gain block where the signal is multiplied by a factor of speed deviation, a signal washout block and a two-stage phase compensation block. The washout block will provide a high-pass filter that passes fast variability caused by the system but blocks slow and steady signals. This is controlled by a time constant, T_W, normally ranging between 1 and 20 seconds. Next, the timing process follows; this is done by advancing (phase leading) the natural delay (phase lag) between the controller input and output in order to synchronise the response appropriately. In practice, the overall aim of the controller is to make a small corrective change in voltage known as ΔVq. This value is added to the main target voltage, Vqref, which is controlled by the slower power flow control

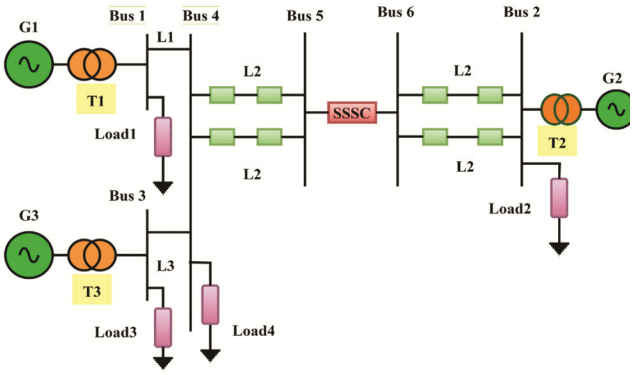

Fig. 1 — MMPS structure with SSSC

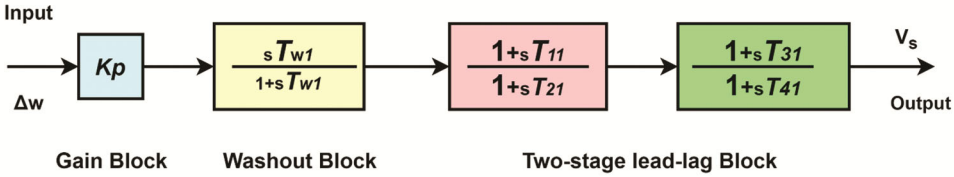

Fig. 2 — Structure of PSS controller

system. Since this primary system is responding to such a slow process, in the cases of sudden, large-scale disturbances, Vqref remains fixed and the damping controller can adjust the SSSC to bring the grid to stabilize within in very short time. Figure 3 shows the structure of SSSC controller.

3 Problem Formation

Using damping controllers, the primary aim of this research work is to decrease the speed deviation of MMPS under various fault and loading scenarios. The primary objective function is the integral time absolute error (ITAE), which is shown in Eq. (1). In this case, Δw_L is defined as a local area speed deviation and is Δw_I defined as an inter-area speed deviation. Table 1 lists the PSS and SSSC controllers' parameters that have to be tuned. The gain constants' top and lower bounds are set at 100 and 2, respectively. In a similar vein, the optimization process sets the upper limit for the time constant at 2, while the lower limit is set at 0.2. The lower and upper limits of both PSS and SSSC are displayed by Eqs. (3) to (6).

$$ITAE = \int_0^{t_s}(\sum|\Delta w_L| + \sum|\Delta w_I|) \quad \ldots (1)$$

Minimize ITAE

$$(\mathrm{K_S}, \mathrm{T_{1S}}, \mathrm{T_{2S}T_{3S}T_{4S}}, \mathrm{K_S}, \mathrm{T_{1S}}, \mathrm{T_{2S}T_{3S}T_{4S}}, \mathrm{K_S}, \mathrm{T_{1S}}, \mathrm{T_{2S}T_{3S}T_{4S}}, \mathrm{K_S}, \mathrm{T_{1S}}, \mathrm{T_{2S}T_{3S}T_{4S}}) \quad \ldots (2)$$

Subjected to

$$\mathrm{K_P^{min}} \le \mathrm{K_P} \le \mathrm{K_P^{max}} \quad \ldots (3)$$

$$\mathrm{K_S^{min}} \le \mathrm{K_S} \le \mathrm{K_S^{max}} \quad \ldots (4)$$

$$\mathrm{T_{xP}^{min}} \le \mathrm{T_{xP}} \le \mathrm{T_{xP}^{max}}; \mathrm{x} = 1,2,3,4 \quad \ldots (5)$$

$$\mathrm{T_{yS}^{min}} \le \mathrm{T_{yS}} \le \mathrm{T_{yS}^{max}}; \mathrm{y} = 1,2,3,4 \quad \ldots (6)$$

where $\mathrm{K_P^{min}}$ and $\mathrm{K_P^{max}}$ represent the PSS gains for lower and upper bounds, respectively. Likewise, $\mathrm{T_{xP}^{min}}$ and $\mathrm{T_{xP}^{max}}$ are used for PSS's time constant, and $\mathrm{T_{yS}^{min}}$ and $\mathrm{T_{yS}^{max}}$ denotes SSSC's time constant. $\mathrm{K_S^{min}}$ and $\mathrm{K_S^{max}}$ represent the SSSC gain constant. The objective function of the multi-machine power system is indicated by Eq. (4). Since each controller has five constants, the objective function for MMPS has four gain constants and sixteen time constants. Using the suggested method, a total of twenty parameters from four controllers have been adjusted.

4 Proposed Algorithm

The proposed GOA method represents the survival activity of gazelles[4]. The gazelles are very lightweight, but they possess a strong sense of smell, hearing, and sight to detect their enemies. These tremendous natural characteristics of these animals protect them from being chased by their predators. Grazing in the absence of a predator and fleeing from a sighted predator comprise this optimization process. The GOA algorithm employed in this work operates in two stages: exploration and exploitation.

4.1 Exploitation

The predators are stalking the gazelles or they are grazing peacefully without being disturbed by the predators. Brownian motion is assumed during this phase for the movement of gazelles. The mathematical model for gazelle behavior is presented in Eq. (7).

$$\text{gazelle}_{j+1} = \text{gazelle}_j + s.R*R_B* .(\text{Elite}_j - R_B* .\text{gazelle}_j) \quad \ldots (7)$$

where gazelle_j is used for the solution of the present iteration and gazelle_{j+1} is used for the solution for next iteration. The speed of gazelles is represented by s. R_B

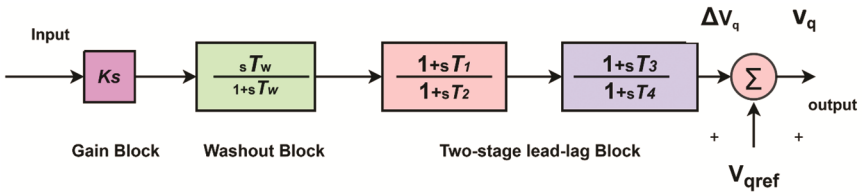

Fig. 3 — Structure of SSSC controller

Table 1 — Gain and time constant of PSS and SSSC controllers

	SSSC	PSS_1	PSS_2	PSS_3
Gain Constant	K_P	K_{S1}	K_{S2}	K_{S3}
Time Constant	$\mathrm{T_{s1}, T_{s2}T_{s3}T_{s4}}$	$\mathrm{T1_{S1}, T1_{S2}T1_{S3}T1_{S4d}}$	$\mathrm{T2_{S1a}, T2_{S2b}T2_{S3b}T2_{S4b}}$	$\mathrm{T3_{Sa1}, T3_{S2b}T3_{S3c}T3_{S4}d}$

represents the Brownian motion which is a vector containing random numbers.

4.2 Exploration

The exploration phase of the algorithm begins immediately upon sighting a predator. Fig. 4(a) represents the gazelles' grazing pattern of exploitation. To warn of danger, gazelles display protective behaviors such tail flicking, foot stomping, or stotting (leaping up to two meters). This 2-meter height is normalized to a value between 0 and 1 for simulation purposes.This phase employs the Lévy flight movement model, which enhances search capability in optimization contexts by combining frequent small steps with occasional long jumps. This movement pattern is visualized in Fig. 4 (b). When the predator is spotted, the gazelle flees, and the predator gives chase. Both the gazelle's run and the predator's pursuit are characterized by a sudden, sharp change in direction represented by the variable μ . In this study, this directional change is assumed to happen in every iteration: the gazelle moves in one direction during odd iterations and the opposite direction during even iterations.

As the gazelle reacts first, its initial flight utilizes the Lévy flight model. The predator's reaction is delayed, so its initial "take-off" run is modeled using Brownian motion before it transitions to the Lévy flight model. The mathematical representation of the gazelle's behavior upon detecting the predator is given in Eq. (8).

$$\overrightarrow{\text{gazelle}_{j+1}} = \overrightarrow{\text{gazelle}_j} + S.\mu.\vec{R} * \vec{R}_L * (\text{Elite}_j - \overrightarrow{R_L} * \overrightarrow{\text{gazelle}_j}) \quad \ldots (8)$$

where S is the gazelle's maximum speed. A vector of random integers based on Levy distributions is represented by R_L. The mathematical model for the predator's pursuit of the gazelle is shown in Eq. (9). equation 10 shows the cumulative factor of the predator.

$$\overrightarrow{\text{gazelle}_{j+1}} = \overrightarrow{\text{gazelle}_j} + S.\mu.CF * \vec{R}_B * (\text{Elite}_j - \overrightarrow{R_L} * \overrightarrow{\text{gazelle}_j}) \quad \ldots (9)$$

$$\text{Where } CF = \left(1 - \frac{\text{iteration}}{\text{Max\_iteration}}\right)^{\left(2\frac{\text{iteration}}{\text{Max\_iteration}}\right)} \quad \ldots (10)$$

Predator success rates, or PSRs, have an impact on the gazelle's capacity to flee, preventing the algorithm from becoming stuck in a local minimum. Equation (11) shows a model of the PSRs effect.

$$\overrightarrow{\text{gazelle}_{j+1}} = \{\overrightarrow{\text{gazelle}_j} + CF[\overrightarrow{LB} + \vec{R} * (\overrightarrow{UB} - \overrightarrow{LB})] * \vec{U} \text{ if } r \leq PSRs \quad \ldots (11)$$

$$\{\overrightarrow{\text{gazelle}_j} + [PSR(1-r) + r](\overrightarrow{\text{gazelle}_{r1}} - \overrightarrow{\text{gazelle}_{r2}})] \text{ else} \quad \ldots (12)$$

where $\vec{U}$ denotes a binary vector, which is constructed by generating a random number r in [0,1] such that $\vec{U}$ =0 if r< 0.34 , otherwise $\vec{U}$ = 1 r1 and r2 are random indexes of the gazelle matrix.

The Fig. 5 illustrates how a Gazelle Optimization Algorithm (GOA) operates, a nature-inspired metaheuristic optimization algorithm inspired by the behaviour and survival strategies of gazelles. The algorithm begins with parameter initialization, where every gazelle corresponds to one possible solution of the optimization problem. That involves their initial

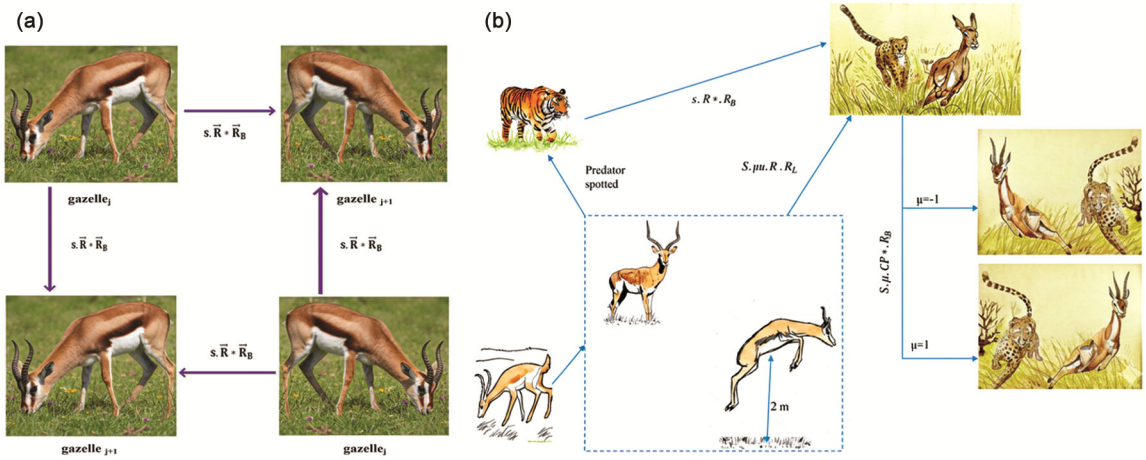

Fig. 4 — (a) The gazelles' grazing pattern of exploitation and (b) Gazelles escaping from the predator signifies exploration

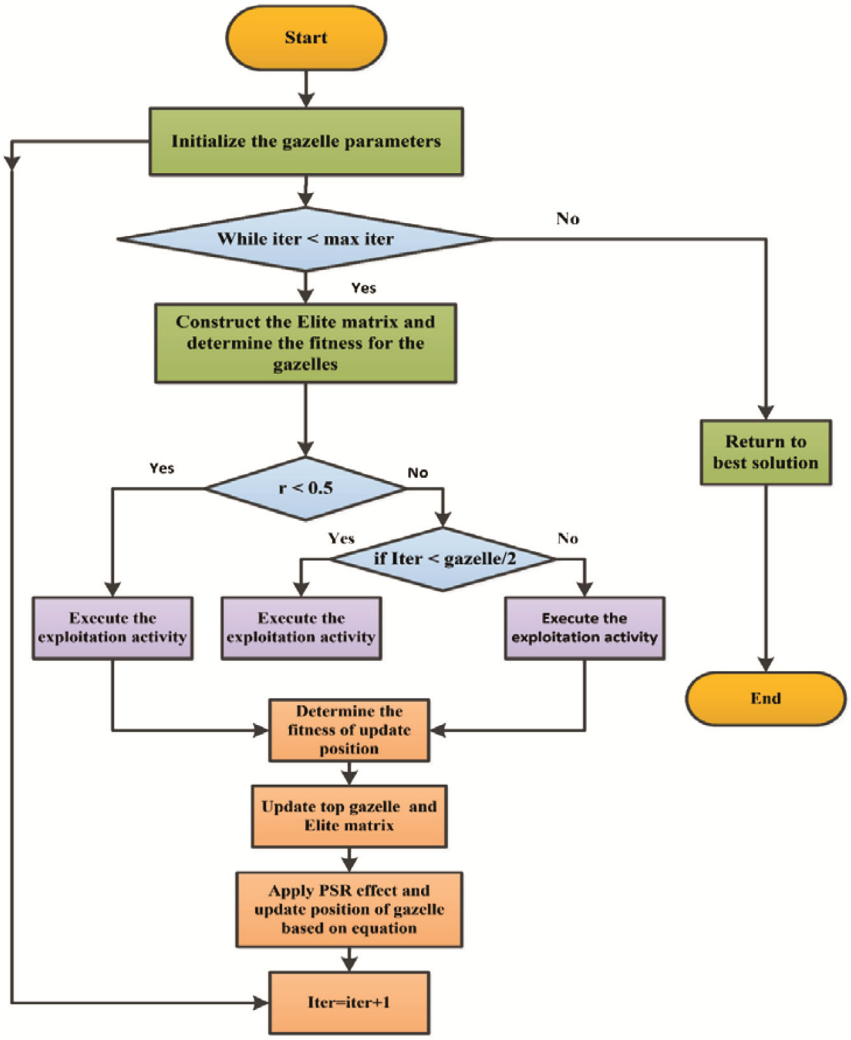

Fig. 5 — Flow chart for the Gazelle optimization algorithm

positions as well as other suitable features. This optimization process then goes in a loop which is repeated till the optimum number of iterations is attained. At every iteration, the algorithm creates an Elite matrix, which holds to the best-performing gazelles and offers the fitness of all the gazelles within the population. On the basis of a random control parameter r r, the algorithm makes the decision of which kind of exploitation strategy to use. If $r < 0.5$ The height of a certain exploitation activity is done to optimize solutions within the promising areas a r 0.5 is achieved. If $r \geq 0.5$ r>0.5, other considerations is made to decipher whether the current iteration in the search process is in the first half of the total search. When it is, one particular exploitation process is performed; otherwise, another variation is utilized. These exploitation attempts are aimed at optimizing solutions by manipulating the position of gazelles to enhance fitness values. Once positions have been updated, the algorithm checks the fitness of the new positions and replaces the top gazelle and Elite matrix in the event of better solutions having been found. An effect is then introduced similar to a Predator Search Response (PSR) effect to simulate natural predator-avoidance behaviours, which promotes exploration and [avoids] premature convergence. The loop is then repeated with a better iteration counter; the loop will repeat itself until the terminating condition is reached. After the loop terminates, the algorithm gives out the best solution that was discovered so far in the course of the search. This as a theoretical framework that enables exploration, exploitation, preservation of an elite solution, and predator-avoidance practices that can be

employed in navigating the search space and solving optimization issues.

5 Performance Analysis of the Proposed Algorithm (GOA)

Whenever we propose a new optimization technique to prove its superiority, a statistical analysis must be performed along with its benchmark function test with other optimization techniques. The suggested GOA and other optimization methods have been executed for 500 iterations with 50 repetitions in this work. The analysis has been performed with both unimodal and multimodal benchmark functions of each algorithm. Unimodal functions only have one global optimum, which are simple to solve and useful for evaluating the exploitation of algorithms, whereas multimodal functions are challenging, have numerous local optima, and consider the exploration of algorithms. Table 2 shows the details of the Benchmark Functions used for performance evaluation with different algorithms. Table 3 shows the Mean± std. Dev values for unimodal and multimodal functions of different optimization techniques starting from F1- F13 function. The unimodal function contains F1 to F7 functions, whereas the multimodal function contains more complex benchmark functions, i.e., F8 to F13 functions. The proposed GOA has been compared with other metaheuristic optimization techniques, i.e SCA[24], MFO[25], and ALO[26]. Figure 6 represents the graphical overview of the proposed work with its problem formulation and its application. Figures 7 -19 show the different benchmark functions of various algorithms in comparison to GOA, starting from F1 to F13, respectively. In the function F1, F2, F3, F4, F7, F8, F10, F11 graph, the proposed GOA gives a better convergence rate than other optimization where as in the functions F5, F9, F12, the convergence graph of GOA is close to the other three algorithms. In Fig.12 and Fig. 19 it can be observed that the proposed technique has weaker convergence characteristics than other optimization algorithms. In the F6 function, MFO has the best convergence rate among others where whereas in the F13 function, ALO leads in faster convergence rate among other techniques. The better convergence characteristics of the GOA in the benchmark test comparison demonstrate its superiority among others.

The non-parametric Wilcoxon signed-rank test (WSRT) is used in place of the paired t-test when the distribution of the data cannot be assumed to be normal. In order to perform the WSRT test, each pair's differences are calculated, their absolute values are ranked, and the ranks are then added together according to their initial positive or negative and equivalent signs. The WSRT is utilized at a 95 % significance level during data review to determine whether a method is superior (+), inferior (-), or equivalent (≈) to the suggested GOA technique.

Table 2 — Benchmark functions used for performance evaluation with different algorithms

Function	Dimension	Range	f_{min}
$f_1(x) = \sum_{i=1}^{n} x_i^2$	30	[-100,100]	0
$f_2(x) = \sum_{i=1}^{n} \mid x_i \mid + \prod_{i=1}^{n} \mid x_i \mid$	30	[-10,10]	0
$f_3(x) = \sum_{i=1}^{n} (\sum_{j-1}^{i} x_j)^2$	30	[-100,100]	0
$f_4(x) = max_i\{\mid x_i \mid, 1 \le i \le n\}$	30	[-100,100]	0
$f_5(x) = \sum_{i=1}^{n} [(x_{i+1} - x_i^2)^2 + (x_i - 1)^2]$	30	[-30,30]	0
$f_6(x) = n \sum_{i=1}^{n} ([x_i + 0.5])^2$	30	[-100,100]	0
$f_7(x) = \sum_{i=1}^{n} i x_i^4 + random[0,1]$	30	[-100,100]	0
$f_8(x) = \sum_{i=1}^{n} -x_i \sin(\sqrt{\mid x_i \mid})$	30	[-500,500]	0
$f_9(x) = \sum_{i=0}^{n} [x_i^2 - 10\cos(2\pi x_i) + 10]$	30	[-5.12,5.12]	0
$f_{10}(x) = -20 \exp\left(-0.2\sqrt{\frac{1}{n}\sum_{i=1}^{n} x_i^2}\right) - \exp(\frac{1}{n}\sum_{i=1}^{n} \cos(2\pi x_i)) + 20 + e.$	30	[-32,32]	0
$f_{11}(x) = \frac{1}{4000}\sum_{i=1}^{n} x_i^2 - \prod_{i=1}^{n} \cos(\frac{x_i}{\sqrt{i}}) + 1$	30	[-600,600]	0
$f_{12}(x) = \frac{\pi}{n}\{10\sin$	30	[-50,50]	0
$(\pi y_1) + \sum_{i=1}^{n-1} (y_i - 1)^2 [1 + 10sin^2(\pi y_{i+1})] + (y_{n-1})^2\} + \sum_{i=1}^{n} u(x_i, 10,100,4)$			
$y_i = 1 + \frac{x_i + 1}{4} \quad u(x_i, a, k, m) = \begin{cases} k(x_i - a)^m & x_i > a \\ 0 & -a < x_i < a \\ k(-x_i - a)^m & x_i < -a \end{cases}$			
$f_{13}(x) = 0.1\{sin^2(3\pi x_1) + \sum_{i=1}^{n} (x_i - 1)^2 [1 + sin^2(3\pi x_i + 1)] + (x_n - 1)^2 [1 + sin^2(2\pi x_n)]\} + \sum_{i=1}^{n} u(x_i, 5,100,4)$	30	[-50,50]	0

Table 3 — Values for unimodal and multimodal functions of various optimization techniques

Function	Mean± std Dev			
	SCA	MFO	ALO	GOA
F1	2.33103E-10 ±6.92289E-10	5.64676E-12 ±1.61079E-11	6.92216E-08 ±1.07521E-07	6.75273E-37 ±4.16144E-36
F2	1.1118E-08 ±2.97411E-08	1.23584E-09 ±3.815756803	0.812428767 ±1.813982986	1.38938E-11 ±9.7195609
F3	0.020921 ±0.048418	435.290276 ±1483.092071	8.692690996 ±1678.7249776	2.32997E-3 ±18.68123765
F4	0.00431E-3 ±0.00693	11.23718E-2 ±12.32247959	12.425678849 ±1.311596069	0.14401E-7 ±0.711802
F5	7456.698499 ±0.438419	7581.207415 ±24321.20751	1736.3376844 ±370.3258346	461.85366 ±0.802701
F6	0.53108 ±0.161174	1.21721E-13 ±5.02147E-12	8.0558E-08 ±1.32729E-07	2.223115 ±0.893109
F7	0.004463 ±0.006431	0.019054852 ±0.013231262	0.04992252 ±0.03670287	0.006593 ±0.007968
F8	-2002.15 ±175.7085	-3179.385849 ±324.4614162	-2057.454575 ±502.0384013	-9519.08 ±962.2345
F9	33.23806 ±7.0907	31.04497428 ±15.5601011	24.35652987 ±11.24824267	4.221531 ±14.81125
F10	0.73073E-1 ±3.4257	0.396085786 ±0.894280129	0.490575055 ±0.916796971	2.39535E-07 ±1.44952E-07
F11	0.1537 ±0.226	0.167223805 ±0.085296817	0.181706645 ±0.076444655	9.97703E-02 ±6.97822E-06
F12	0.5125 ±0.057	0.573317949 ±1.946490019	4.662307128 ±3.079835689	0.157954 ±0.020071
F13	0.3631 ±0.084	0.059022096 ±0.258355628	0.004723209 ±0.007413081	1.52425 ±0.41925

Table 4 displays the findings for WSRT results for various algorithms. The result table indicates that the suggested GOA is better than the other three approaches (SCA, MFO and ALO). Based on the WSRT test, the negative indications in the maximum case concluded that the suggested GOA performs superior to others.

The mean ranks of four distinct methods—SCA, MFO, ALO, and GOA—are displayed in this bar chart in Fig. 20. These methods are the main outcomes of non-parametric statistical tests like the Friedman test, which are frequently followed by a post-hoc test like the Nemenyi hypothesis test. The picture visualizes the mean ranks, which is a necessary initial step for a Nemenyi post-hoc analysis. According to the Friedman-Nemenyi test, the algorithm that has the lowest mean rank is superior to the other algorithms. It is clearly observed from the Fig. 20 GOA, MFO performed significantly better than SCA and ALO. The proposed GOA has the minimum mean rank (15.67), followed by MFO (17.58), SCA (32.33) and ALO (32.44), which proves the effectiveness of the proposed techniques.

Table 4 — Wilcoxon signed-rank test comparison for different algorithms with the proposed GOA method, showing superior (+), inferior (−), or equivalent (≈)

	SCA	MFO	ALO
F1	-	-	≈
F2	≈	-	-
F3	-	+	-
F4	-	-	+
F5	≈	-	-
F6	-	≈	-
F7	+	-	-
F8	-	-	+
F9	-	-	-
F10	-	≈	≈
F11	≈	-	-
F12	-	-	≈
F13	-	+	+

6 Results and Discussion

The suggested GOA approach has improved system stability by adjusting the MMPS damping controllers' parameters. MATLAB 2023 has been used to develop and simulate the proposed test system. The detailed structure of the simulation is

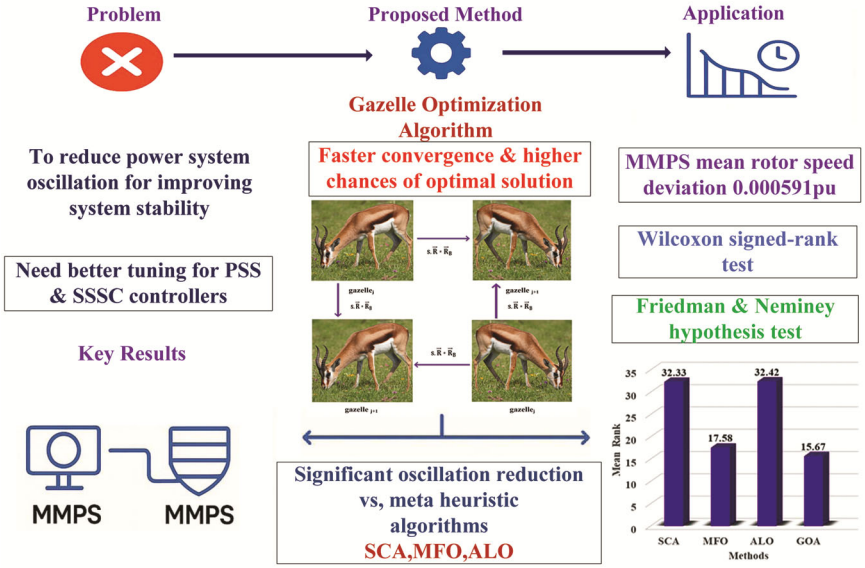

Fig. 6 — Graphical overview of proposed work with GOA

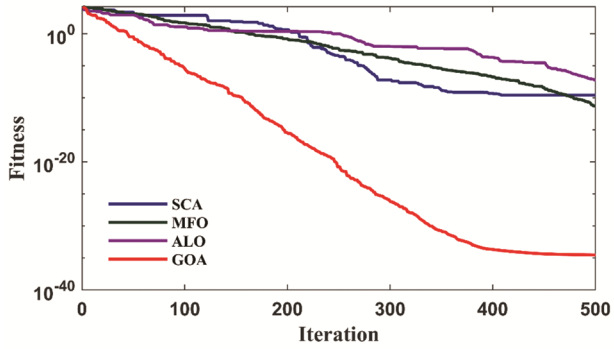

Fig. 7 — Convergence characteristics of optimization algorithms for F1 function

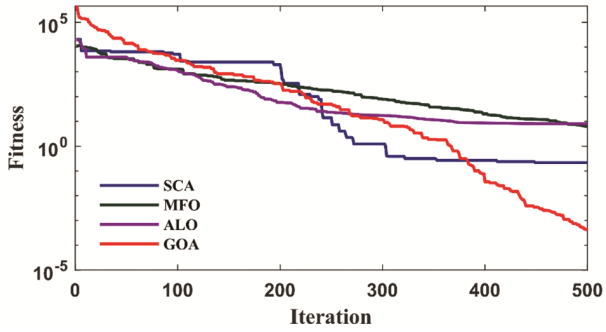

Fig. 9 — Convergence characteristics of optimization algorithms for F3 function

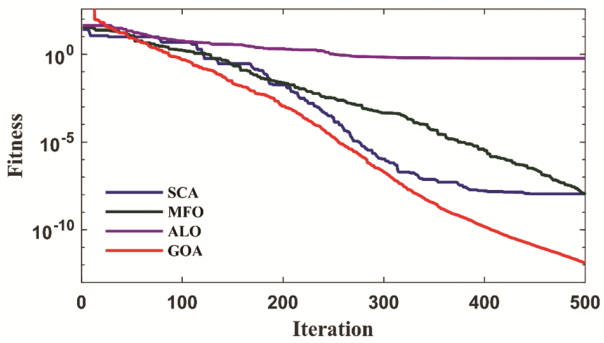

Fig. 8 — Convergence characteristics of optimization algorithms for F2 function

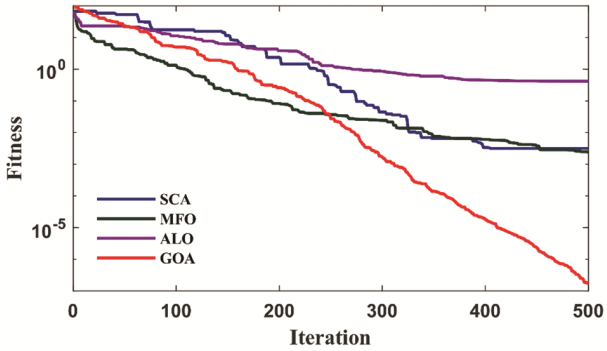

Fig. 10 — Convergence characteristics of optimization algorithms for F4 function

shown in Fig. 21. The three machines, named as M1, M2, M3, are installed with their corresponding transformer. The three-phase fault, which is applied between bus no 6 and 2, is self-clearing in nature. Once the fault is cleared, the system regains its original position. After running the simulation, various parameters such as speed deviation, tie line power, and injected voltage by the SSSC of the system are taken into consideration. For comparison purposes, different optimization techniques named as

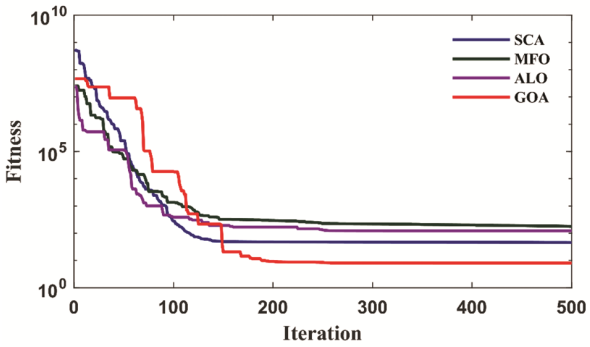

Fig. 11 — Convergence characteristics of optimization algorithms for F5 function

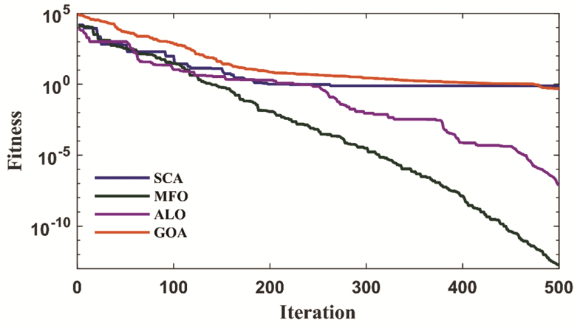

Fig. 12 — Convergence characteristics of optimization algorithms for F6 function

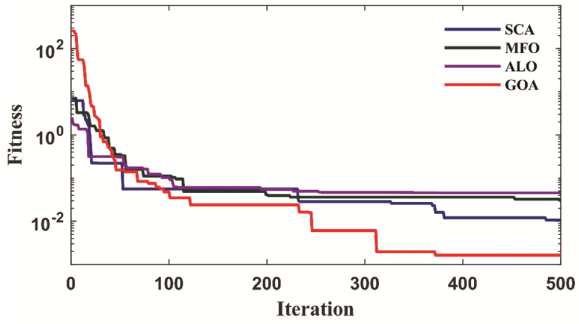

Fig. 13 — Convergence characteristics of optimization algorithms for F7 function

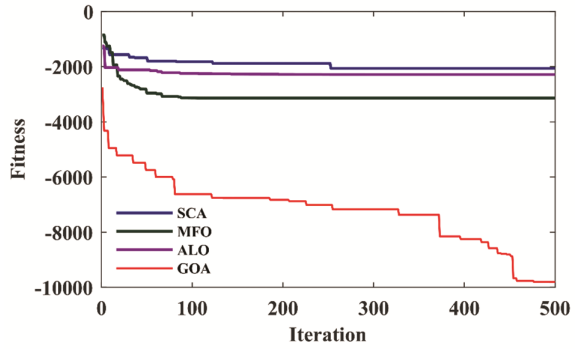

Fig. 14 — Convergence characteristics of optimization algorithms for F8 function

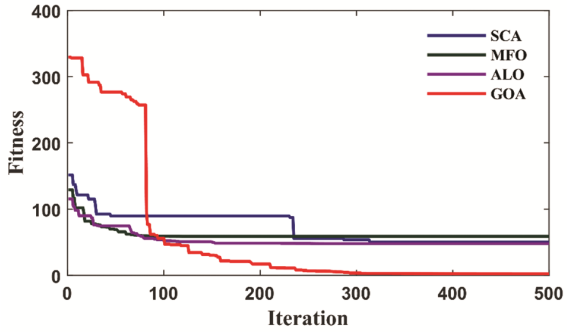

Fig. 15 — Convergence characteristics of optimization algorithms for F9 function

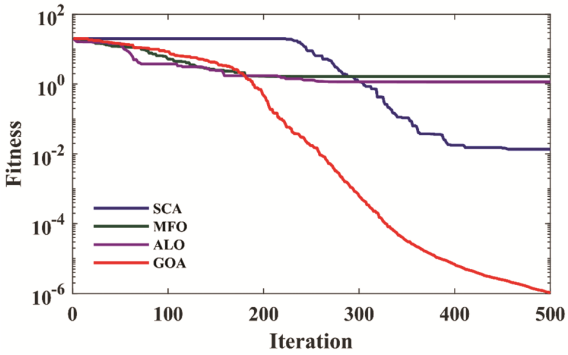

Fig. 16 — Convergence characteristics of optimization algorithms for F10 function

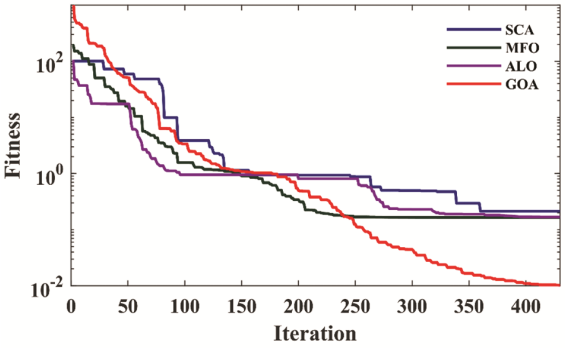

Fig. 17 — Convergence characteristics of optimization algorithms for F11 function

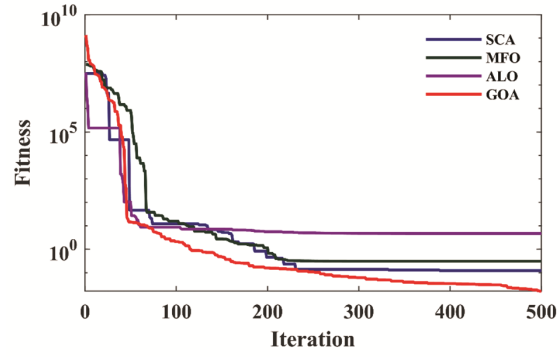

Fig. 18 — Convergence characteristics of optimization algorithms for F12 function

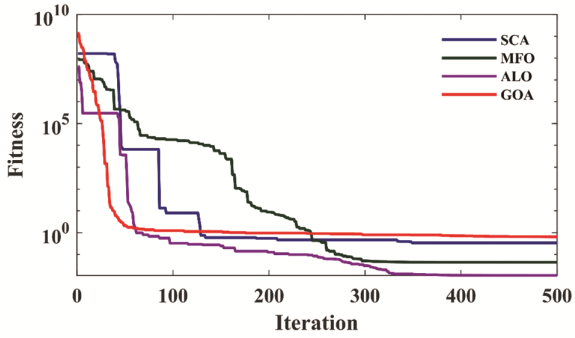

Fig. 19 — Convergence characteristics of optimization algorithms for F13 function

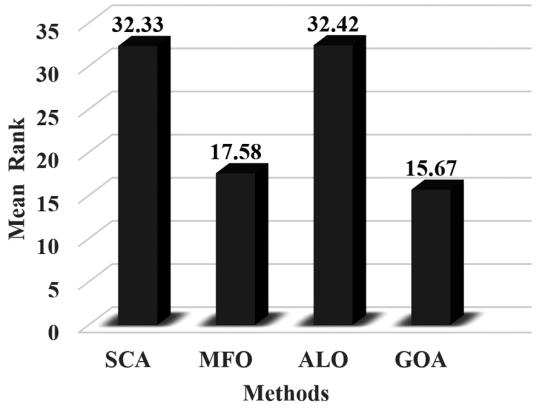

Fig. 20 — Mean rank comparison of different optimization algorithms

SCA, MFO, ALO are considered with their simulation result. Figure 22 shown the speed deviation between machine 1 and 2, whereas Fig. 23 shows the speed deviation between machines 2 and 3. Speed deviation

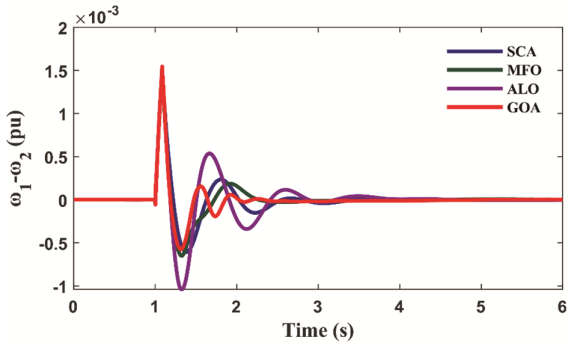

Fig. 22 — Speed deviation between machine 1 and 2

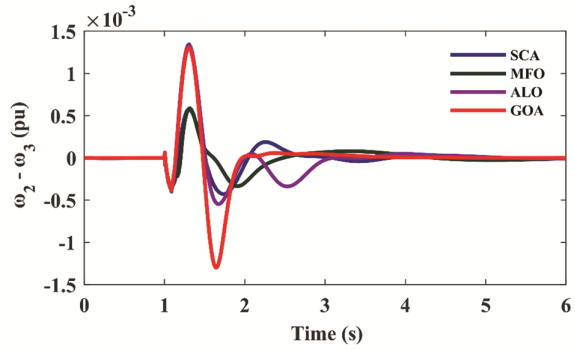

Fig. 23 — Speed deviation between machine 2 and 3

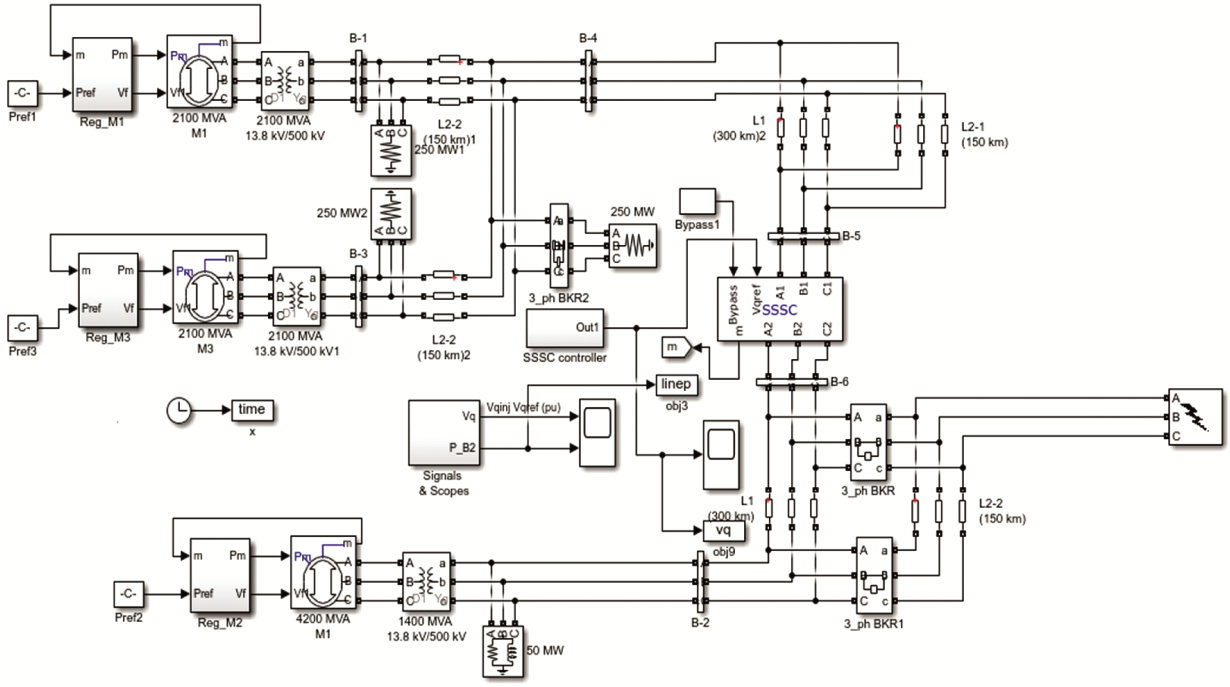

Fig. 21 — Matlab Simulink model of MMPS system

of machine 1 and 3 is displayed by Fig. 24. The tie line power and SSSC injected voltage are shown by Figs. 25 and 26, respectively. Table 5 shows the fitness value (mean and standard deviation) of different optimization methods. From Table 5, the fitness value of the GOA technique is 0.000591, which is minimum than other optimizer which shows the effectiveness of the proposed technique. The fitness value obtained from the proposed GOA has been compared with existing work[7], in which the fitness value was 0.000601 using the slap swarm algorithm, which is higher than the GOA optimized value. The fitness value of GOA is significantly lower than the MGWPSO-based fitness value for the MMPS system i.e., 0.000902 in S.K[17]. Optimized parameter values using different optimization methods for both PSS and SSSC are given in Table 6.

Figure 22 shows a comparative analysis of GOA with different optimization algorithms, which provides the most effective control for stabilizing the system after a disturbance. This graph illustrates the speed deviation between machine 1 and machine 2 of the multimachine power system, following a disturbance. It compares the performance of four different optimization algorithms, SCA, MFO, ALO,

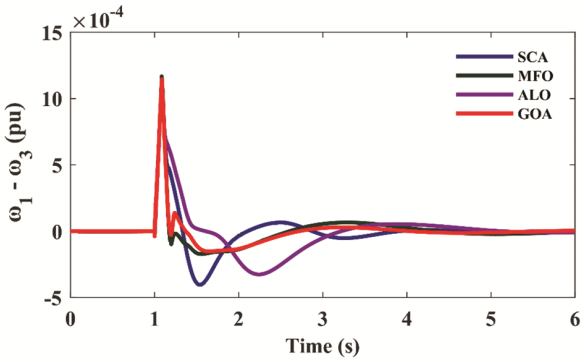

Fig. 24 — Speed deviation between machine 1 and 3

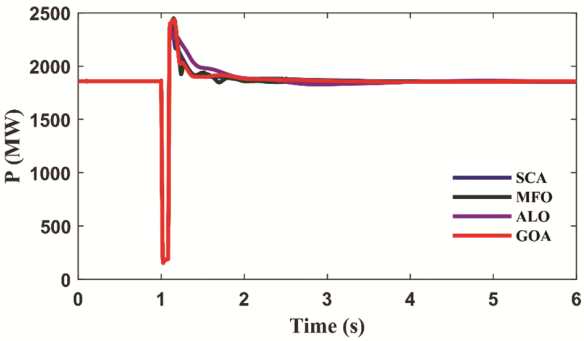

Fig. 25 — Tie-line power

Table 5 — Fitness value of different optimization algorithms for MMPS system

	SCA	MFO	ALO	GOA
Fitness value	0.001198± 0.000197	0.000971± 0.000199	0.001419± 0.000403	0.000591± 0.000126

Table 6 — Optimized controller parameter values for PSS and SSSC of MMPS system for different algorithms

Controller	parameters	Methods			
		SCA	MFO	ALO	GOA (PROPOSED)
SSSC	K_S	43.947	83.18	48.172	80
	T_{s1}	1.0665	0.66688	1.1789	1.4275
	T_{s2}	1.4324	0.64373	1.7661	0.01
	T_{s3}	2	0.38771	1.9377	0.40243
	T_{s4}	0.36712	0.3266	1.0566	1.0951
PSS_1	K_{P1}	0.9617	99.962	82.91	18.846
	T_{11}	0.2932	0.022101	0.88053	0.24896
	T_{21}	0.1369	1.249	1.643	0.01
	T_{31}	0.013038	0.05516	0.92086	0.25642
	T_{41}	0.019481	2	0.076529	0.01
PSS_2	K_{P2}	64.598	5.3527	21.573	45.781
	T_{11}	0.01	1.999	1.1473	2
	T_{21}	0.01	2	1.0523	1.0223
	T_{31}	0.028931	0.79214	1.0503	0.27591
	T_{41}	0.021215	0.10147	0.41472	0.28985
PSS_3	K_{P3}	0.19875	79.089	18.032	1.4066
	T_{11}	0.01638	1.6171	1.4111	0.01
	T_{21}	0.027698	1.8871	1.8177	0.026892
	T_{31}	0.024339	1.2895	0.92836	0.01
	T_{41}	0.022292	1.976	1.7862	2

and the proposed GOA, used to tune a controller. Where x shows the time, and the y-axis represents speed deviation in per units. It can be concluded from the above figure that the proposed algorithm (GOA) gives better stability than other algorithms as it minimizes frequency deviations and settles the fastest.

The transient stability response of a multi-machine power system for different optimized controllers is compared in Fig. 23, which displays the difference in rotor speed between machines 2 and 3 after a disturbance at about one second. The four curves illustrate the performance achieved when the coordinate controllers are tuned using various optimisation algorithms, including SCA, MFO, ALO, and GOA. The GOA (red line) shows the largest initial oscillation and settles down after the disturbance very quickly in comparison to the others. From the result, it can be concluded that the proposed GOA gives better stability performance followed by MFO, SCA and ALO.

Figure 24 shows the rotor speed deviation comparison of machines 1 and 3 with the different optimization techniques compared to others. From the figure, it has been clearly visualized that the proposed GOA approach gives better stability performance than SCA.MFO and ALO optimization.

Figure 25 displays the stability of Tie-line power for various optimization techniques, where the power (P) output, measured in megawatts, and the time frame is 6 seconds following a major fault or disturbance that occurs at a second. The graph compares the stability analysis of four distinct metaheuristic optimization techniques. Before the fault, the power level is stable at approximately 1850 MW. When the fault is applied, the power sharply drops, followed by an immediate, overshoot peaking near 2500 MW. The suggested GOA approach (red line) displays the most pronounced initial peak and the most rapid, yet oscillatory, transient behaviour as it attempts to restore the equilibrium quickly and stabilize the system than others. All four methods successfully dampen the oscillations, converging back to the required steady-state power level within 3 to 4 seconds. The conclusion can be drawn from the figure that the GOA approach gives better stability performance in terms of tie-line power compared to other three optimizations.

The dynamic response of injected voltage (Vq) under four distinct algorithms SCA, MFO, ALO, and the suggested GOA, is shown in Fig. 26. All controllers return to their pre-disturbance steady state of Vq = 0 pu after the disturbance occurs at t=1s. From the figure, it is clearly seen that the recommended GOA-based controller has a better stability response, showing little overshoot and a quick settling time with minimal oscillations. The SCA, MFO, and ALO controllers, on the other hand, exhibit noticeable transient variations with large overshoots and undershoots, suggesting a less damped and more oscillatory reaction to the system malfunction. From the analysis, it has been concluded that the GOA-based coordinate controller has the most effective damping characteristics and robustness to maintain system voltage stability.

This convergence graph, illustrated in Fig. 27, compares four optimization algorithms—SCA, MFO, ALO, and GOA on their ability to find the best solution (lowest "fitness" value) over several iterations. The GOA algorithm (red line) is the clear winner, as it converges the fastest (in under 15 iterations) and achieves the lowest fitness score, indicating it found the most optimal solution. The other algorithms were either slower to find a solution or settled on a less optimal result within 50 iterations.

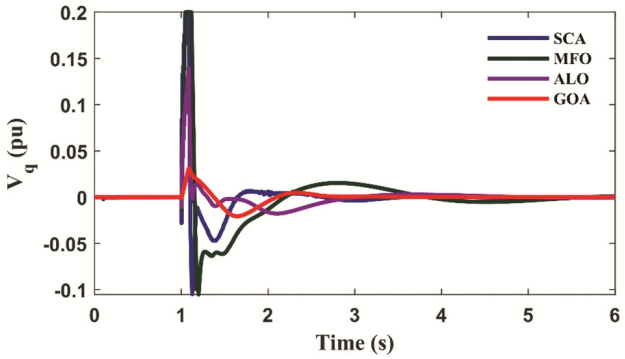

Fig. 26 — Injected voltage by SSSC

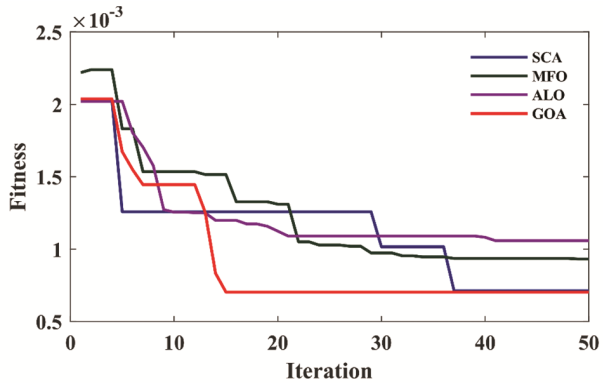

Fig. 27 — Comparison of the convergence graph for different optimization techniques

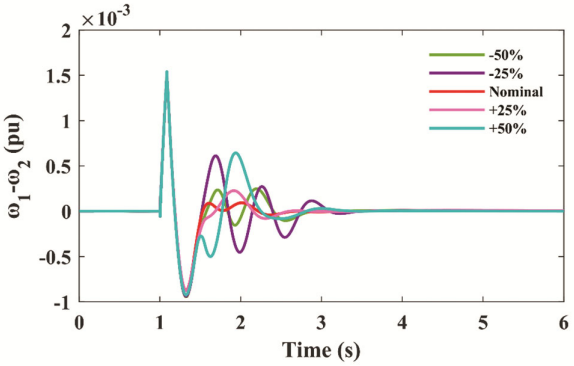

Fig. 28 — Speed deviation response for M1 & M2 with SSSC controller gain variation

6.1 Controller Performance Analysis (Sensitivity Analysis) with the Proposed GOA

The sensitivity analysis for the proposed GOA has been displayed in Fig. 28, In this analysis, the speed deviation response of machines 1 and 2 has been analyzed by varying the gain of the SSSC controller. From Table 5, we obtained the SSSC gain constant 80; however, by varying the gain to ±25 % and ±50 % in the controller parameters, we observed a change in rotor speed deviation as well as system oscillation. Increasing SSSC gains to 100 and 120, which are displayed in the pink and light blue lines, respectively. Decreasing the SSSC gain to -25 % (40) and -50 % (60), which are shown in purple and green lines, respectively, where the nominal value is marked with a red line with a gain value of 80. Five coloured lines indicate how the system responds to the change of the key control parameter of the system by changing it out of its nominal value. The initial transient generates a huge swing in speed; the subsequent oscillations should be damped in order to keep the generation of the generators on track. The most rapid decay and the lowest oscillations happen in case the parameter is increased or maintained at the nominal value (in red and pink). This points to great damping and strength. On the other hand, a smaller parameter (green and purple lines) leads to bigger and more persistent oscillations, and the damping is worse. So, from Fig. 28, it can be concluded that the nominal value and 25 % increment gain value have better stability performance than other gain variation parameters. The variation of the SSSC controller gain results in varying the oscillation of the system, proving the flexibility of the proposed controller.

7 Conclusion

A coordinated design for SSSC and PSS damping controllers was proposed to enhance the dynamic stability of power systems. The controller parameters were optimally tuned using the Gazelle optimization algorithm, with the primary objective of effectively mitigating low-frequency oscillations. The tuned controller parameters have been applied to Multi-Machine Power System (MMPS) environments, and the performance is being analysed by considering different parameters such as speed deviation, SSSC injected voltage and tie line power. A detailed comparative study with other three more recent optimization algorithms proved that GOA performs better in terms of optimum solutions, rate of convergence and stability. Friedman and Nemenyi tests were also used to statistically check the validity of these results with 13 standard benchmark functions, and in all cases, the GOA technique has the lowest level of mean rank, which validates its effectiveness. The Wilcoxon signed-rank test also confirms the superiority of the proposed technique in comparison to others. The result analysis and observation affirm that the proposed GOA-based coordinate controller is a highly effective and practical solution for enhancing power system stability, justifying its potential for implementation in real-world power networks to maintain stability under diverse and challenging operating conditions. However, with some sophisticated controller tuning with an advanced optimization technique may give superior stability performance which is the future extension of this work.

Appendix

List of Abbreviations

GOA – Gazelle Optimization Algorithm
WSRT – Wilcoxon Signed-Rank Test
MMPS – Multimachine Power System
SSSC – Static Synchronous Series Compensator
PSS – Power System Stabilizer
SCA – Sine Cosine Algorithm
MFO – Moth Flame Optimization
ALO – Ant Lion Optimizer

List of Symbols

$\Delta\omega$ – deviation in rotor speed.
Δw_I – inter-area speed deviation
Δw_L – local-area speed deviation
Vq – Injected Voltage
K_P^{min} – Lower limits for PSS gains

K_P^{max} – Upper limits for PSS gain
K_S^{min} – Lower limits for SSSC gains
K_S^{max} – Upper limits for SSSC gains

References

1 Kundur P, *Power system stability control*, 10 (1) (2007) 1.
2 Shea J J, Hingorani N G & Gyugyi L, *IEEE Electr Insul Mag*, 18 (1) (2002) 46.
3 Khadanga R K, Das D & Panda S, *J Electr Comp Eng*, 2024 (1) (2024) 4590764.
4 Agushaka J O, Ezugwu A E & Abualigah L, *Neural Comput Appl*, 35 (5) (2023) 4099.
5 Bhattacharya K, Nanda J & Kothari M L, *Int J Electr Power Energy Syst*, 19 (7) (1997) 58.
6 Mihalič R & Papič I, *Electr Power Syst Res*, 45 (1) (1998) 65.
7 Kar M K, *Int J System Assur Eng Manag*, 14 (6) (2023) 2136.
8 Sahoo S K, Kar M K, Kumar S & Mahanty R N, *J Electr Eng*, 19 (2025)1.
9 Ain Q, Jamil E, Hameed S & Naqvi K H. *Austr J Electr Electr Eng*, 17 (1) (2020) 56.
10 Ali E S, *Int J Electr Power Energy Syst*, 61 (2014) 683.
11 Cai L J & Erlich I, *IEEE Trans Power Syst*, 20 (1) (2005) 294.
12 Sahoo S K, Kar M K, Kumar S & Mohanty R N. Int Conf on Electric Power and Renewable Energy (Springer Nature Singapore), May 2024 pp. 315-329.
13 Khadanga R K & Satapathy J K, *Int J Electr Power Energy Syst*, 71 (2015) 262.
14 Kar M K, Kumar S, Singh A K & Panigrahi S, *Int Trans Electr Energy Syst*, 31 (11) (2021) 13058.
15 Juneja K, *IETE J Res*, 68 (6) (2022) 4437.
16 Du W, Dong W, Wang Y & Wang H, *IEEE Trans Power Syst*, 36 (4) (2020) 3475.
17 Kar M K, Kumar S, Singh A K, Panigrahi S & Cherukuri M, *Int Trans Electr Energy Syst*, 2022 (1) (2022) 5339630.
18 Devarapalli R, Bhattacharyya B, Sinha N K & Dey B, *ISA trans*, 109 (2021) 152.
19 Kar M K, Singh A K, Kumar S & Rout B, *J Inst Eng Ind B*, 105 (1) (2024) 77.
20 Verdejo H, Pino V, Kliemann W, Becker C & Delpiano J, *Energies*, 13 (8) (2020) 2093.
21 Qin S, Zeng H, Sun W, Wu J & Yang J, *Electronics*, 13 (8) (2024) 1580.
22 Sahoo S K, Kar M K, Kumar S & Mahanty R N, *Measure*, 13 (2025) 119723.
23 Diao Q, Xie C, Yin Y, Lee H & Yang H, *Cluster Comput*, 28 (10) (2025) 643.
24 Mirjalili S, *Knowl based syst*, 96 (2016) 120.
25 Mirjalili S, *Knowl based syst*, 89 (2015) 228.
26 Kumar R, Singh R & Ashfaq H, *Comp Electr Eng*, 83 (2020) 106589.